Fabrication of Nano-Structured TiO$_2$ Coatings using a Microblast Deposition Technique

Kevin. A. McDonnell[1,2], Niall. J. English[2], Charlie. P. Stallard[1], Mahfujur Rahman[2],

Denis. P. Dowling [1,2*]

[1]School of Mechanical and Materials Engineering, University College Dublin, Belfield, Dublin 4, Ireland

[2] The SEC Strategic Research Cluster and the Centre for Synthesis and Chemical Biology, School of Chemical and Bioprocess Engineering, University College Dublin, Belfield, Dublin 4, Ireland

*Corresponding Author

School of Mechanical and Materials Engineering, University College Dublin, Belfield, Dublin 4, Ireland. T: + 353-1-716 1747, F: + 353-1-283 0534, E: denis.dowling@ucd.ie

Keywords: Titanium Dioxide, Solar, Microblast, Agglomerated Nanoparticles, Spraying

Abstract

Micron thick Titanium Dioxide (TiO$_2$) coatings exhibiting a nano-structured, anatase, meso-porous structure were successfully deposited across a range of polymer, conductive glass and metallic substrates at low velocities using a microblasting technique. This process was conducted at atmospheric pressure using compressed air as the carrier gas and commercially available agglomerated nano particles of TiO$_2$ as the feedstock. An examination of the effect of impact kinetics on the agglomerated powder before and after deposition was undertaken. A further examination of the coating microstructure along with photocurrent density measurements before and after thermal treatments was explored. Owing to the low temperature and velocity of the powder during deposition no change in phase of the powder or damage to the substrate was observed. The resulting TiO$_2$ coatings exhibited relatively good adhesion on both titanium and FTO coated glass substrates with coating thickness of approximately 1.5 μm. Photo-catalytic performance was measured under solar simulator illumination using a photo-electrochemical cell (PEC) with a 5 fold increase in performance observed after thermal treatment of the TiO$_2$ coated substrates. Microblasting was demonstrated to be a rapid and cost effective method for the deposition of nano-structured, photo-catalytic, anatase TiO$_2$ coatings.

1. Introduction

Titanium Dioxide (TiO_2) coatings have found uses in a variety of fields from self cleaning and antimicrobial surfaces to solar applications [1]. Due to these numerous applications, there has been a significant level of research into the method of deposition of TiO_2. This has led to the development of various deposition processes such as sputtering [2-4], sol gel [5] and thermal spraying [6-8] amongst others.

Whilst the large scale fabrication of TiO_2 coatings using powder by thermal spray means is commonplace, a difficulty arises in the deposition of these coatings for photo-catalytic purposes. The anatase crystalline form is the most photoactive phase of TiO_2 [9] and generally present up to temperatures of ~900 °C [10]. In thermal spray depositions however, coatings are formed above this phase transition temperature as molten and semi-molten particles adhere and solidify on the surface with an irreversible transformation into the less photoactive rutile crystallite phases [11]. A further detrimental effect of the high deposition temperatures are changes to the physical and chemical composition of the substrate material.

Cold spray provides a solution to the problematic temperature issue of the thermal spray deposition methods by replacing the high temperatures with high particle velocities > 400 m/s [12]. Within this process particulate adhesion results from the plastic deformation of the ductile feedstock material as it impacts the substrate at velocities beyond their critical velocity. The critical velocity is denoted as the point at which the probability of the powder sticking to the substrate is greater than that of eroding it [13]. Helium is often used as the process gas in these systems due to its lower molecular weight when compared to air, resulting in a faster gas stream and hence a higher resultant particle velocity [14]. Helium, however, is expensive and as such makes it prohibitive to extend its use to a large scale industrial setting. Brittle materials such as TiO_2 are also problematic to deposit using cold spray. These materials suffer extensively from bow shock deceleration before impact with the surface causing fragmentation of the powder and instead of undergoing plastic deformation, they mechanically embed themselves into the substrate [10].

This paper explores a potential solution to the problems highlighted for other deposition methods for the creation of nano-structured, anatase, TiO_2 coatings through the use of a simple, quick and cost effective powder coating technology called microblasting. While agglomerated TiO_2 nano-particles have been used previously to deposit such photo-catalytic coatings, these depositions were conducted using either He as a process gas, in evacuated

chambers or a combination of both [15-17]. Kim et al, similar to this study used compressed air as their process gas, however, the deposition was once again undertaken in an evacuated chamber [18].

To the best of our knowledge this paper presents results for the first time on nano-structured TiO_2 coatings created using agglomerated nano-particles at ambient pressure and temperature using compressed air as a carrier gas on a range of substrates.

2. Methodology

2.1 Materials

Commercially available spray dry agglomerated TiO_2 nano-particles (Inframat Advanced Materials) of pure anatase crystalline structure with 40 nm primary particle size and 40 μm average agglomerate size were used as the feedstock for the deposition process. Pure titanium sheets (99.6%, supplied by Goodfellow Cambridge Ltd.) of size 20 mm × 15 mm × 0.5 mm and FTO coated glass were used as the substrate. Prior to use, the metallic substrates were rinsed in a pickling solution (3% HF + 30% HNO_3 + 67% de-ionized H_2O) for 1 min to remove any native oxide before being ultrasonically cleaned in methanol followed by acetone for 5 min each.

2.2 Deposition

The microblast process involves the acceleration of micron sized particles by compressed air through a circular nozzle (COMCO MB2520) with an aperture of 1.5 mm. The depositions were conducted in a chamber at atmospheric pressure and ambient temperature. The nozzle was traversed across the substrate at 10 mm/s, at a standoff distance of 20 mm and an input pressure of 90 PSI using a programmable Staubli RX60 robotic arm to ensure control. After each deposition, before characterisation of the coating loosely bound TiO_2 particles were removed by ultrasonically cleaning the samples in deionised water for 3 minutes.

2.3 Post Deposition Thermal Treatment

Post deposition thermal treatments were carried out as a means to improve the inter-particle connectivity and the adhesion of the coating to the substrate and also to remove binding chemicals used in the manufacture of the agglomerated powder. Two methods of

sintering were explored and compared. In the first method, samples were placed in a preheated Carbolite CWF 1200 chamber furnace for 5 minutes at 500°C, removed and allowed to air cool. For the second method a circumferential antenna plasma (CAP) microwave (2.45 GHz) system which has been described elsewhere [19] was employed. The chamber was pumped down to 0.1 mbar and an argon and oxygen atmosphere of 10:1 introduced. The microwave discharge was then ignited to form a plasma ball around the samples located in the centre of the chamber. Input powers of 2.4 kW were provided from a Mugge microwave power supply. Deposition temperatures were measured using a LASCON QP003 two-colour pyrometer and maintained at 500°C. The samples were exposed to the plasma for the same time period as the furnace so a direct comparison could be made.

2.4 Characterisation

The degree of crystallinity and the phase composition of the coatings were examined by a Siemens D500 X-ray diffractometer (XRD) operating at 40 kV and 30 mA with Cu Kα radiation at a wavelength of 0.1542 nm. The scan was conducted in 2θ mode and spanned across a range of 20° to 80° with a step resolution of 0.02°.

Particle size distribution of the powder was conducted using a Sympatec HELOS laser diffraction based Particle Size Analyser (PSA). The measurement was repeated in triplicate using purified deionised water as the dispersion medium.

Light absorption was measured using an Analytik Jena Specord 210 UV-Vis spectrometer configured in reflectance mode using an integrating sphere attachment. The scan was conducted over a spectral range of 290 to 800 nm.

Fourier transform infrared spectroscopy (FTIR) measurements were carried out on the agglomerated TiO_2 powder as received, post deposition and post thermal treatment using a Bruker Vertex-70 system. The sample chamber was purged by N_2 gas before the scans were obtained. Spectra were collected in the range of $400 - 4000$ cm^{-1} using a spectral resolution of 4 cm^{-1}.

The morphology and surface roughness of the sample surface was examined using a Wyko NT1100 Optical Profilometer operating in vertical scanning interferometry (VSI) mode with a 50× lens. Roughness measurements are quoted as Ra which is the arithmetic average of the roughness profile.

Further surface analysis and cross sectional investigations of the coating were carried out using a FEI Quanta 3D FEG DaulBeam[TM] (FEI Ltd, Hillsboro, USA) focused ion beam/scanning electron microscope (FIB/SEM) system. The deposited coatings were sputter coated with platinum prior to analyses using an Emitech K575X sputter coating unit to prevent surface charging by the electron beam. The TiO_2 power was examined by placing the power onto a conducting adhesive pad and they were then examined directly using a Hitachi SEM.

The photocurrent density, which is proportional to the rate of water splitting reaction to hydrogen and oxygen on the photo cathode and photo anode respectively, was used as a means of assessing water splitting in a PEC cell [20]. The measurements of photocurrent were carried out using a custom-made photo-electrochemical cell (PEC), a Gamry G300 potentiostat and a Newport 450 W (xenon arc lamp) solar simulator. Simulated sunlight (AM 1.5) was supplied through a fused quartz glass window onto the front side of the photoelectrode surface at a measured intensity of 1000 W m^{-2}. The PEC cell consists of three electrodes: a working electrode (TiO_2 coating), a counter platinum electrode and a reference electrode immersed in an electrolyte aqueous solution of 0.05 M NaOH. Light Intensity was measured by a photodiode power meter. The flat band potential was obtained from the I_p versus E_{app} curve and presumed to be approximately equal to the potential value at the onset of the anodic photocurrent.

2.5 Coating Adherence

The adhesive strength of the microblasted coatings was determined according to an adhesive tape test based on a modified ASTM D6862 standard [21]. One end of a 10mm wide section of non elastic tape with a failure load of 8.2 N/10 mm was applied to the sample using a 40 N load roller. The other end of the tape was attached to a tensile testing machine and exposed to an increasing tensile load. Measurements were undertaken using a 1 kN load cell.

3. Results and Discussion

The main objective of this study was to evaluate the use of the microblast technique for the deposition of anatase nano-structured photo-catalytic TiO_2 coatings directly from the

oxide powder and to assess whether any change in crystalline phase took place during deposition. To garner a deeper understanding into the deposition process a study of the effect of surface impact on the agglomerated nano-powder was conducted prior to an examination of the coatings being undertaken.

3.1 Effect of Substrate Impact on Agglomerated Particles

Characterisation of the powders was carried out both pre and post deposition. These are denoted "as received" and "post deposition" respectively. The post deposition powder samples were obtained by removing loosely adhered TiO_2 powder by tapping the coated samples. This was carried out prior to the sample undergoing a sonication step for the full removal of loose material. Figure 1 displays the XRD and the absorption spectra for the TiO_2 powder as received and post deposition. The XRD spectra show no change in peak position or intensities between samples indicating that no change in the anatase phase due to the deposition process had occurred. This result was further supported by the absorption plots which show no significant change in position.

The SEM images (Figure 2) of particulate structure before and after deposition illustrates a more fragmented and jagged powder in the post deposition image (right), when compared to the as received powder (left). This change in particulate structure is likely to be due to the emanating shockwaves which permeate though the agglomerate on impact with the substrate and also through the particle-particle collisions which occur within the deposition stream [22, 23].

Particle size analysis measurements further support this fragmentation with a shift to lower particle sizes clearly observable after deposition. The sharp cut off at 500 nm in figure 3 for the post deposition sample is due to the cut off resolution of the device. The high distribution value at this point indicates that a large proportion of particulates are smaller than 500 nm.

Figure 4 compares the FTIR spectra of TiO_2 particulates before and after coating deposition and also after thermal treatment of the as received powder. Peaks centered at 1390 and 1548 cm^{-1}, present in the as received and post deposition samples are thought to be from a

titanium-acetate complex used the production of the nano-agglomerate powder [24]. As noted previously, the microblast process is low temperature technique and is unable to burn off this acetate complex. The presence of such a complex is detrimental to any photo-activity and hence a thermal treatment of the as received powder at 500°C for 5 minutes was undertaken. A reduction and complete removal of these peaks was observed post thermal treatment. The broad band centered at 750 cm^{-1} corresponds to lattice vibrations in the TiO_2 molecule [24]. There was no apparent change to this peak before and after thermal treatment, indicating that the molecular structure of the powder had not been significantly altered. Post deposition, there is a slight augmentation in the shape of the peak and this is possibly due to the irregularly shaped particles created from surface impaction. The chemical integrity of the nano-powder does not appear to be significantly altered by this microblasting technique.

3.2: Effect of thermal treatments on coating morphology and photocurrent

In preliminary studies the ability of the microblast technique to deposit micron thick TiO_2 coatings onto polymer, metal and glass substrates was successfully demonstrated as illustrated in Figure 5. The focus of this paper is the investigation of the properties of the oxide coating deposited on both titanium sheet and Fluorine Tin Oxide (FTO) coated glass substrates.
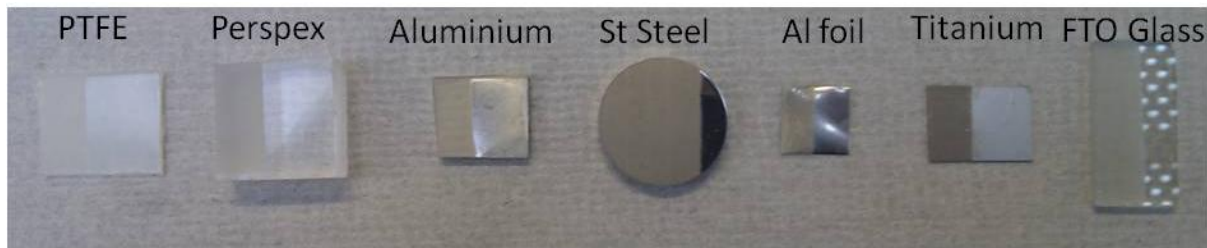

Figure 5: Micron thick TiO_2 coatings were deposited onto polymer (PTFE, Perspex), metal (stainless steel, titanium, aluminium sheet and foil) as well as fluorine tin oxide coated glass substrates. The photograph shows the coated and uncoated regions on each material.

SEM images of the TiO_2 coating demonstrated a very similar powder grain structure on both the FTO and titanium metal substrates. From the SEM image Figure 6 (A) and the cross sectional image shown in figure 7, complete coverage of the titanium substrate is observed. The particle size of the coating was seen to compare directly with the un-agglomerated particle size of the feedstock, ~40nm. It was noted that these smaller particles were preferentially adherent on the substrate. There are two possible explanations for this, the first is by critical velocity; unlike larger particles within the distribution, the smaller particles

were travelling at a velocity exceeding the critical velocity and adhere to the substrate rather than eroding it [15]. A second potential explanation could be due to electrostatic and Van der Waal surface charge effects [23]. The impacts of particles which do not adhere to the substrate result in activation and build up of charge on the substrate. This charge along with the charge built up by the powder through particle-particle and particle-tube interactions is large enough for the smaller particles to be electrostatically held in place on the substrate. These restrained particles are then subjected to impacting forces from successive particles in the stream which effectively "hammer" the initial particles into the surface resulting in adherence and coating growth. A topographical image of the surface over a larger area is shown in optical profilometry image in Figure 5-B. Surface roughness (R_a) values are given in Table 1.

Figure 8 shows two images of the FIB cross section of an as deposited TiO_2 coating, one at 80,000× and 150,000×. The coating exhibits a meso-porous structure with a significant level of interconnectivity between the particles. At higher magnification, the substrate-coating interface is shown. Just to note that there was no evidence for deformation of the substrate by the microblasting process. The variation in the titanium metal surface roughness in Figure 8 for example is associated with the roughness (R_a) of the as-received substrate which as detailed in Table 1 is 344 nm. The lack of surface damage from the impacting TiO2 particles would indicate that the mechanism of coating adhesion is associated with an electrostatic deposition process [23], rather than a mechanical embedding. There may also be an element of fracture on the outer surface of the TiO_2 nano-particles exposing Ti^+ bonds which act as a nucleus for interfacial bonding and enhancing adhesion. A better approximation of photocurrent density values, hence photo catalytic performance were obtained by measuring numerous as deposited coatings Samples were found to have a relatively low average value of 57 μAcm^{-2}.

In order to improve the photocurrent density, an increase in the interconnectivity of the particles was required to facilitate an easier transfer of electrons from the substrate to the surface of the coating. In this study the effect of two alternative post deposition thermal treatments were investigated. Firstly the use of a resistance furnace treatment and secondly the heating effect of a microwave plasma [24]. Samples A and B in Figure 9 represent two different magnifications of the same sample which was treated in a furnace at 500°C for 5 minutes. A densification of the coating and indication of a significant level of 'necking'

between the particulates was concluded based on their relatively good adhesive bond strength and higher photocurrent densities compared with the as-deposited coatings, as discussed in later sections. A similar observation was obtained for samples treated within the microwave plasma for the same treatment time, however a higher level of densification appeared to have occurred through a noticeable reduction in coating thickness as illustrated in subset images C and D in Figure 9.

Microwave plasma works on the principle of volumetric heating rather than the conductive heating method obtained in the furnace and results in more localised heating of the samples. Microwaves are also more penetrative and therefore a more uniform thermal treatment throughout the depth of the coating was obtained. Although denser, the coating was observed to still be meso-porous with the cross section images indicating good interconnectivity of particles. Better particle-substrate connectivity was also observed for both sintering methods post thermal treatment. A possible explanation could be due to localised heating effects of the metallic substrate on the interfacial particles. These particles become partially molten on thermal treatment, solidify on cooling, improving substrate adherence.

Table 1 presents results for surface roughness, thickness and photocurrent density for all samples "as deposited" and "thermally treated". All values represent averaged values across at least 3 samples with typical standard deviations of 15 nm, 10 $\mu A/cm^2$ and 150 nm for roughness, photocurrent density and coating thickness respectively. The photo current values reported in this article are at an applied voltage of 1.23 V vs RHE. The flatband potential of furnace and microwave sinterted electrlode were calculated to be - 0.87418 V vs SCE (0.176 V vs RHE) and -0.89833 V vs SCE (0.152 V vs RHE) respectively. The photocurrent results obtained are comparable to PVD coatings of similar thickness measured under the same illumination conditions [25]. They are however lower than the mA / cm^2 values that Yang and Fan et al achieved through their vacuum cold spray deposition approach which involved thicker (10-20 μm) coatings [26, 27].

The roughness measurements shown in Table 1 provide information on the average surface roughness R_a, a significant further issue with respect to performance will be the meso-porous underlying structure. Roughness and photocurrent density was observed to increase after thermal treatment, with coating thickness decreasing. The microwave plasma

method of thermal treatment was observed to yield higher photocurrent densities compared to that obtained with the furnace treatment.

Further deposition trials were carried out to examine the effect of multiple passes on coating thickness. It was observed that the thickness of the coating did not increase above a maximum of ~1.5μm as the number of deposition passes was increased. This is possibly due to an adhesion / erosion mechanism i.e, the larger, slower velocity particles within the depostion stream eroding rather than sticking to the previously adhered coating.

3.3 Coating Adhesion

A test was undertaken based on a modified ASTM D6862 standard to examine if the thermal treatments had increased the interfacial bond strength between the substrate and the coating. At least three measurements were made for each sample and the average measurement is shown in Figure 10. The tape used in the experiment was non-elasticated with a failure load of 8.2 N per 10 mm. A 10 mm wide tape was applied under a fixed load to each substrate and connected at the other end to a force sensor. The tape was pulled at a constant rate and the resulting force required to remove the tape from the surface measured. The tape removed a significant portion of the as-deposited TiO_2 coating; however both thermally treated samples exceeded the failure load of the tape. For these samples the failure occurred within the tape and not between the coating and the tape. This experiment confirms the observation based on the cross sectional images in Figure 8, where better particle adhesion between the coating and substrate was observed after thermal treatment.

One of the major advantages of the microblast process is the ability to deposit coatings on delicate substrates such as FTO glass without causing significant damage to the conducting FTO layer. This is illustrated for the thermally treated micron thick coating on the FTO coated glass in Figure 11. Due to a lower surface area of the substrate, shown by lower surface roughness statistics of ~7 nm, the bonding of the TiO_2 particles to the smoother substrate is not as good. Photocurrent measurements taken on the FTO gives marginally lower results than that of the Titanium substrate but the trends between thermal treatment methods is the same.

4. Conclusions

Photo-catalytic micron thick TiO_2 coatings were successfully deposited onto both titanium metal and FTO coated glass substrates from approx. 40 μm TiO_2 nanoparticle agglomerates, using a microblast technique. A threshold thickness was observed of ~1.5μm with increasing numbers of deposition passes resulting in no further coating thickness growth. No appreciable damage to the FTO coated glass or titanium substrates was observed with the microblast deposition process. The use of furnace and microwave plasma treatments was investigated as a means of enhancing the adhesion and inter-particle connectivity of the TiO_2 coatings. Both thermal treatments were successful in this regard with the metal oxide successfully passing the tape test. The TiO_2 coatings which were plasma treatment however yielded a higher particle packing density, which resulted in photocurrent density measurements 5 times greater than their as deposited counterpart and slightly higher to those which were furnace treated. It was concluded from this study that the microblast technique combined with the use of agglomerated nanoparticles, has the potential as a relatively low cost, scalable processing technique for the deposition of TiO_2 coatings onto both titanium and FTO coated glass substrates.

5. References

1. Bak, T., et al., *Photo-electrochemical hydrogen generation from water using solar energy. Materials-related aspects.* International Journal of Hydrogen Energy, 2002. **27**(10): p. 991-1022.
2. Biswas, S., et al., *Study of photocatalytic activity in sputter-deposited Cr-TiO_{<FONT SIZE='-1'>2</FONT>} thin film.* physica status solidi (a), 2008. **205**(8): p. 2023-2027.
3. Dholam, R., et al., *Efficient indium tin oxide/Cr-doped-TiO2 multilayer thin films for H2 production by photocatalytic water-splitting.* International Journal of Hydrogen Energy. **35**(18): p. 9581-9590.
4. Radecka, M., et al., *Study of the TiO2-Cr2O3 system for photoelectrolytic decomposition of water.* Solid State Ionics, 2003. **157**(1-4): p. 379-386.
5. Pan, C.-C. and J.C.S. Wu, *Visible-light response Cr-doped TiO2-XNX photocatalysts.* Materials Chemistry and Physics, 2006. **100**(1): p. 102-107.

6.   Toma, F.L., et al., *Comparative study on the photocatalytic decomposition of nitrogen oxides using TiO₂ coatings prepared by conventional plasma spraying and suspension plasma spraying.* Surface and Coatings Technology, 2006. **200**(20): p. 5855-5862.

7.   Toma, F.L., et al., *Comparison of the photocatalytic behavior of TiO 2 coatings elaborated by different thermal spraying processes.* Journal of Thermal Spray Technology, 2006. **15**(4): p. 576-581.

8.   Yang, G.J., et al., *Dominant microstructural feature over photocatalytic activity of high velocity oxy-fuel sprayed TiO2 coating.* Surface and Coatings Technology, 2007. **202**(1): p. 63-68.

9.   Wold, A., *Photocatalytic properties of titanium dioxide (TiO2).* Chemistry of Materials, 1993. **5**(3): p. 280-283.

10.   Yamada, M., et al., *Fabrication of Titanium Dioxide Photocatalyst Coatings by Cold Spray.* Journal of Solid Mechanics and Materials Engineering, 2009. **3**(2): p. 210-216.

11.   Berger-Keller, N., et al., *Microstructure of plasma-sprayed titania coatings deposited from spray-dried powder.* Surface and Coatings Technology, 2003. **168**(2–3): p. 281-290.

12.   Alkhimov, A.P., et al., *Gas-dynamic spraying method for applying a coating*, 1994, Google Patents.

13.   Assadi, H., et al., *Bonding mechanism in cold gas spraying.* Acta Materialia, 2003. **51**(15): p. 4379-4394.

14.   Ning, X.J., J.H. Jang, and H.J. Kim, *The effects of powder properties on in-flight particle velocity and deposition process during low pressure cold spray process.* Applied Surface Science, 2007. **253**(18): p. 7449-7455.

15.   Burlacov, I., et al., *Cold gas dynamic spraying (CGDS) of TiO₂(anatase) powders onto poly (sulfone) substrates: Microstructural characterisation and photocatalytic efficiency.* Journal of Photochemistry and Photobiology A: Chemistry, 2007. **187**(2): p. 285-292.

16.   Yang, G.J., et al., *Influence of Annealing on Photocatalytic Performance and Adhesion of Vacuum Cold-Sprayed Nanostructured TiO 2 Coating.* Journal of Thermal Spray Technology, 2007. **16**(5): p. 873-880.

17.   Yang, G.J., et al., *Low temperature deposition and characterization of TiO₂ photocatalytic film through cold spray.* Applied Surface Science, 2008. **254**(13): p. 3979-3982.

18.   Kim, Y.H., et al., *Deposition of TiO₂ layers for dye-sensitized solar cells using nano-particle deposition system.* Current Applied Physics, 2011. **11**(1): p. S122-S126.

19.   McConnell, M.L., et al., *High pressure diamond and diamond-like carbon deposition using a microwave CAP reactor.* Diamond and Related Materials, 2002. **11**(3-6): p. 1036-1040.

20.   Khan, S.U.M., M. Al-Shahry, and W.B. Ingler, *Efficient Photochemical Water Splitting by a Chemically Modified n-TiO2.* Science, 2002. **297**(5590): p. 2243-2245.

21.   standerdisation, E.c.f.s., *ECSS-Q-ST-70-13C.* ESA Requirements and Standards Division, 2008.

22.   Gao, P.-H., et al., *Influence of substrate hardness on deposition behavior of single porous WC-12Co particle in cold spraying.* Surface and Coatings Technology, 2008. **203**(3–4): p. 384-390.

23.   Klinkov, S.V., V.F. Kosarev, and M. Rein, *Cold spray deposition: Significance of particle impact phenomena.* Aerospace Science and Technology, 2005. **9**(7): p. 582-591.

24.   Sui, R., A.S. Rizkalla, and P.A. Charpentier, *FTIR Study on the Formation of TiO2 Nanostructures in Supercritical CO2.* The Journal of Physical Chemistry B, 2006. **110**(33): p. 16212-16218.

25.   Rahman, M., et al., *Effect of Doping (C or N) and Co-Doping (C+N) on the Photoactive Properties of Magnetron Sputtered Titania Coatings for the Application of Solar Water-Splitting.* Journal of Nanoscience and Nanotechnology, 2012. **12**(6): p. 4729-4735.

26.   Fan, S.Q., et al., *Fabrication of Nano-TiO 2 Coating for Dye-Sensitized Solar Cell by Vacuum Cold Spraying at Room Temperature.* Journal of Thermal Spray Technology, 2007. **16**(5): p. 893-897.

27.   Yang, G.J., et al., *Influence of gas flow during vacuum cold spraying of nano-porous TiO2 film by using strengthened nanostructured powder on performance of dye-sensitized solar cell.* Thin Solid Films, 2011.